SEECCM III
3rd South-East European Conference on Computational Mechanics-
an ECCOMAS and IACM Special Interest Conference
M. Papadrakakis, M. Kojic, I. Tuncer (eds.)
Kos Island, Greece, 12–14 June 2013

SOLUTION OF VISCOPLASTIC FLOWS WITH THE FINITE VOLUME / MULTIGRID METHOD

Alexandros Syrakos[1], Georgios C. Georgiou[2], and Andreas N. Alexandrou[3]

[1] Oceanography Centre, University of Cyprus
PO Box 20537, 1678 Nicosia, Cyprus
e-mail: syrakos.alexandros@ucy.ac.cy

[2] Department of Mathematics and Statistics, University of Cyprus
PO Box 20537, 1678 Nicosia, Cyprus
e-mail: georgios@ucy.ac.cy

[3] Department of Mechanical and Manufacturing Engineering, University of Cyprus
PO Box 20537, 1678 Nicosia, Cyprus
e-mail: andalexa@ucy.ac.cy

Keywords: Finite Volume Method, Viscoplastic Flows, Papanastasiou Regularisation, Multigrid, Lid-driven Cavity

Abstract. *We investigate the performance of the finite volume method in solving viscoplastic flows. The square lid-driven cavity flow of a Bingham plastic is chosen as the test case and the constitutive equation is regularised as proposed by Papanastasiou [J. Rheol. 31 (1987) 385-404]. The numerical results obtained for Bingham numbers up to 10 and Reynolds numbers up to 5000 compare favourably with reported results obtained through other methods. The effects of the Reynolds and Bingham numbers are also investigated. It is shown that the convergence rate of the standard SIMPLE pressure-correction algorithm, which is used to solve the algebraic equation system that is produced by the finite volume discretisation, severely deteriorates as the Bingham number increases, with a corresponding increase in the non-linearity of the equations. Using the SIMPLE algorithm in a multigrid context [Syrakos & Goulas, Int. J. Numer. Methods Fluids 52 (2006) 1215-1245] dramatically improves convergence, although the multigrid convergence rates are not as high as those for Newtonian flows.*

1 INTRODUCTION

Viscoplastic materials behave as solids at low stress levels, but flow when the stress exceeds a critical value, the *yield stress*, τ_y. Materials which are suspensions of particles or macromolecules, such as pastes, gels, foams, drilling fluids, food products, and nanocomposites, can be considered to fall into this category. Bingham plastics are the simplest viscoplastic materials, which exhibit a linear stress to rate-of-strain relationship once the material yields. The constant of proportionality of this linear relationship is called the *plastic viscosity*, μ. Thus, the Bingham constitutive equation is the following:

$$\begin{cases} \dot{\boldsymbol{\gamma}} \;=\; \mathbf{0}\,, & \tau \le \tau_y \\ \boldsymbol{\tau} \;=\; \left(\frac{\tau_y}{\dot{\gamma}} + \mu\right)\dot{\boldsymbol{\gamma}}\,, & \tau > \tau_y \end{cases} \tag{1}$$

where $\boldsymbol{\tau}$ is the stress tensor and $\dot{\boldsymbol{\gamma}}$ is the rate of strain tensor, $\dot{\boldsymbol{\gamma}} \equiv \nabla\mathbf{u} + (\nabla\mathbf{u})^{\mathrm{T}}$, $\mathbf{u}$ being the velocity vector. The magnitudes of these two tensors are $\tau = [\boldsymbol{\tau}\!:\!\boldsymbol{\tau}/2]^{1/2}$ and $\dot{\gamma} = [\dot{\boldsymbol{\gamma}}\!:\!\dot{\boldsymbol{\gamma}}/2]^{1/2}$.

The discontinuity of the Bingham constitutive equation poses significant difficulties to numerical solution methods. A way to overcome this difficulty is to approximate the Bingham constitutive equation by a regularised constitutive equation which treats the whole material as a fluid and is valid throughout the domain, approximating the solid regions by locally assigning a very high value to the viscosity. Such methods can be implemented with minimal modification to Newtonian flow solvers. One of the most successful regularisation approaches is that by Papanastasiou [1], which has been adopted in the present work. The regularisation is achieved through the introduction of an exponential term, so that the constitutive equation (1) is replaced by the single equation, applicable throughout the material,

$$\boldsymbol{\tau} \;=\; \left[\frac{\tau_y}{\dot{\gamma}}\{1 - \exp(-m\dot{\gamma})\} \;+\; \mu\right]\dot{\boldsymbol{\gamma}} \tag{2}$$

where m denotes the stress growth parameter, which needs to be "sufficiently" large. Using this approximation, we adapted the finite volume method described in [2] to enable it to simulate flows of Bingham plastics. The method was applied successfully in the case of creeping flows in [3]. In the present work, the method is applied also to non-zero Reynolds number flows, with the Reynolds number reaching values as high as 5000.

The finite volume method (FVM) is a popular method for solving fluid flows, employed by many general-purpose CFD solvers. However, there are a limited number of published results on the use of the finite-volume method to solve Bingham flow problems. Neofytou [4] used a FVM in conjunction with the SIMPLE algebraic solver [5] to simulate the lid-driven cavity flow of various non-Newtonian fluids, including a Papanastasiou-regularised Bingham plastic at relatively low yield stress values. Turan and co-workers [6] also used a commercial FVM/SIMPLE code employing the bi-viscosity model in order to simulate natural convection of a Bingham plastic in a square cavity. The FVM was also used to solve flows of a Casson fluid through a stenosis [7] and through a sudden expansion [8], at rather low yield-stress values. Also, de Souza Mendes et al. [9] and Naccache and Barbosa [10] used the FVM in order to simulate viscoplastic flow through an expansion followed by a contraction.

The present method is tested on the popular lid-driven cavity problem: A square cavity of side L is filled with a fluid which is set to motion by the lid of the cavity which moves with a tangential velocity U. Two are the relevant dimensionless numbers for this flow: the Reynolds

number, which, in the case of Bingham fluids, is defined in terms of the plastic viscosity,

$$Re \equiv \frac{\rho U L}{\mu} \tag{3}$$

and the Bingham number Bn, defined as

$$Bn \equiv \frac{\tau_y L}{\mu U} \tag{4}$$

The lid-driven cavity problem has also been used to test methods for solving viscoplastic flows. The aforementioned work of Neofytou [4] is, to the authors knowledge, the only one which employed the finite volume method. However, since it is restricted to very low Bingham numbers, it was not used in the present study for purposes of validation. To validate the present results, the works of Vola et al [13] and Prashant and Derksen [14] were used. Vola et al [13] used an augmented Lagrangian method [15], which obviates the need for regularisation, combined with finite elements. Prashant and Derksen [14] used the lattice-Boltzmann method and a bi-viscosity model (O'Donovan and Tanner [16]) where solid regions are approximated by fluids of a constant high viscosity.

The governing equations are summarised in Section 2, the finite volume method and the algebraic solver are described in Section 3, and the results of the lid-driven cavity simulations are given in Section 4. The paper ends with some conclusions in Section 5.

2 GOVERNING EQUATIONS

The flow is assumed to be steady-state, two-dimensional, incompressible, and isothermal. By scaling the fluid velocity by U, and the pressure and stress by $\mu U/L$, the continuity and momentum equations can be written in the following dimensionless forms:

$$\nabla \cdot \mathbf{u} = 0 \tag{5}$$

$$Re \cdot \mathbf{u} \cdot \nabla \mathbf{u} = -\nabla p + \nabla \cdot \boldsymbol{\tau} \tag{6}$$

where $\mathbf{u}$ is the dimensionless velocity of the fluid, p is the dimensionless pressure, and $\boldsymbol{\tau}$ is the dimensionless stress tensor, which is calculated according to the dimensionless form of the Papanastasiou constitutive equation,

$$\boldsymbol{\tau} = \left[\frac{Bn}{\dot{\gamma}} \{1 - \exp(-M\dot{\gamma})\} + 1 \right] \dot{\boldsymbol{\gamma}} \tag{7}$$

where M is the dimensionless stress growth parameter, defined as:

$$M \equiv \frac{mU}{L} \tag{8}$$

Equations (5), (6) and (7) together with the no-slip wall boundary conditions fully determine the flow problem which is solved numerically.

The Papanastasiou regularisation (7) corresponds to a dimensionless apparent viscosity of

$$\eta = \frac{Bn}{\dot{\gamma}} \{1 - \exp(-M\dot{\gamma})\} + 1 \tag{9}$$

The higher the value of M, the better (7) approximates the actual Bingham constitutive equation, $\boldsymbol{\tau} = [Bn/\dot{\gamma}+1]\dot{\boldsymbol{\gamma}}$, in the yielded regions of the flow field ($\tau < Bn$), and the higher the apparent viscosity is in the unyielded regions, making them behave approximately as solid bodies. For practical reasons though, M must not be so high as to cause problems to the numerical methods used to solve the above equations.

3 NUMERICAL METHOD

The finite volume method employed here is based on that described in [2]. The domain is discretised into 512×512 square control volumes of equal size. Coarser grids are constructed by removing every second grid line from the immediately finer grid. The velocity components, pressure, and viscosity are stored at control volume centres. The convective and viscous fluxes are discretised using 2^{nd}-order central differences. The mass fluxes are discretised using momentum interpolation as described in [11], to suppress pressure oscillations. The resulting algebraic system is solved using the SIMPLE algorithm, with the only modification being that at the start of every SIMPLE iteration the viscosity is updated according to (9), using the current estimate of the velocity field. To accelerate convergence, SIMPLE is used in a multigrid framework. Due to the high degree of nonlinearity of the problem, the standard multigrid algorithm fails to converge except at small Bingham numbers, $Bn < 0.5$. To overcome this problem, we applied the modification suggested by Ferziger and Peric [12]; on coarse grids the viscosity is not updated according to (9), but it is interpolated (restricted) from the immediately finer grid and held constant within the multigrid cycle. Therefore the viscosity is updated only on the finest grid, which means that the procedure is not purely multigrid, but it has single-grid features. This technique was observed to slow down the multigrid convergence by a small amount, but it makes the algorithm more robust and capable of achieving convergence up to high Bingham numbers (depending also on the value of M). Other measures that were found necessary in order to achieve convergence are the following: a large number of pre- and post- smoothing steps should be used (4 or more, depending on the Bn number); a number of additional SIMPLE iterations (e.g. 5 – 10) may have to be performed on the finest grid between multigrid cycles; very small values of the underrelaxation factor a_p for pressure should be used in the SIMPLE smoother (e.g. 0.01); also, relatively small values should be assigned to the velocity underrelaxation factor, $a_u \approx 0.3$, for $Re \geq 2000$; and the coarse grid corrections may have to be underrelaxed by a constant $\alpha_{MG} \approx 0.9$ prior to prolongation to the fine grid.

4 NUMERICAL RESULTS

The lid-driven cavity problem has been solved for Reynolds numbers up to 5000, and for Bingham numbers up to 10. Unless otherwise stated, the results were obtained on the 512×512 grid, using $M = 400$.

Figures 1 – 3 describe the evolution of the flow field as the Reynolds number increases, for Bn = 0, 1, and 10, respectively. The main characteristics of the flow field are a main vortex near the centre of the cavity, and (usually) two unyielded zones, one at the bottom of the cavity and one near the vortex centre, the latter not being in contact with the cavity walls. The unyielded zones, which are of course absent for $Bn = 0$, grow in size as the Bingham number increases. At the bottom of the cavity, for $Bn = 1$, there appear two unyielded zones, one at each of the lower corners, which merge into a single zone as Bn increases. The unyielded zones at the bottom of the cavity are motionless, as they touch the motionless sides of the cavity and have to obey the no-slip condition. The figures however reveal extremely weak vortices at the lower

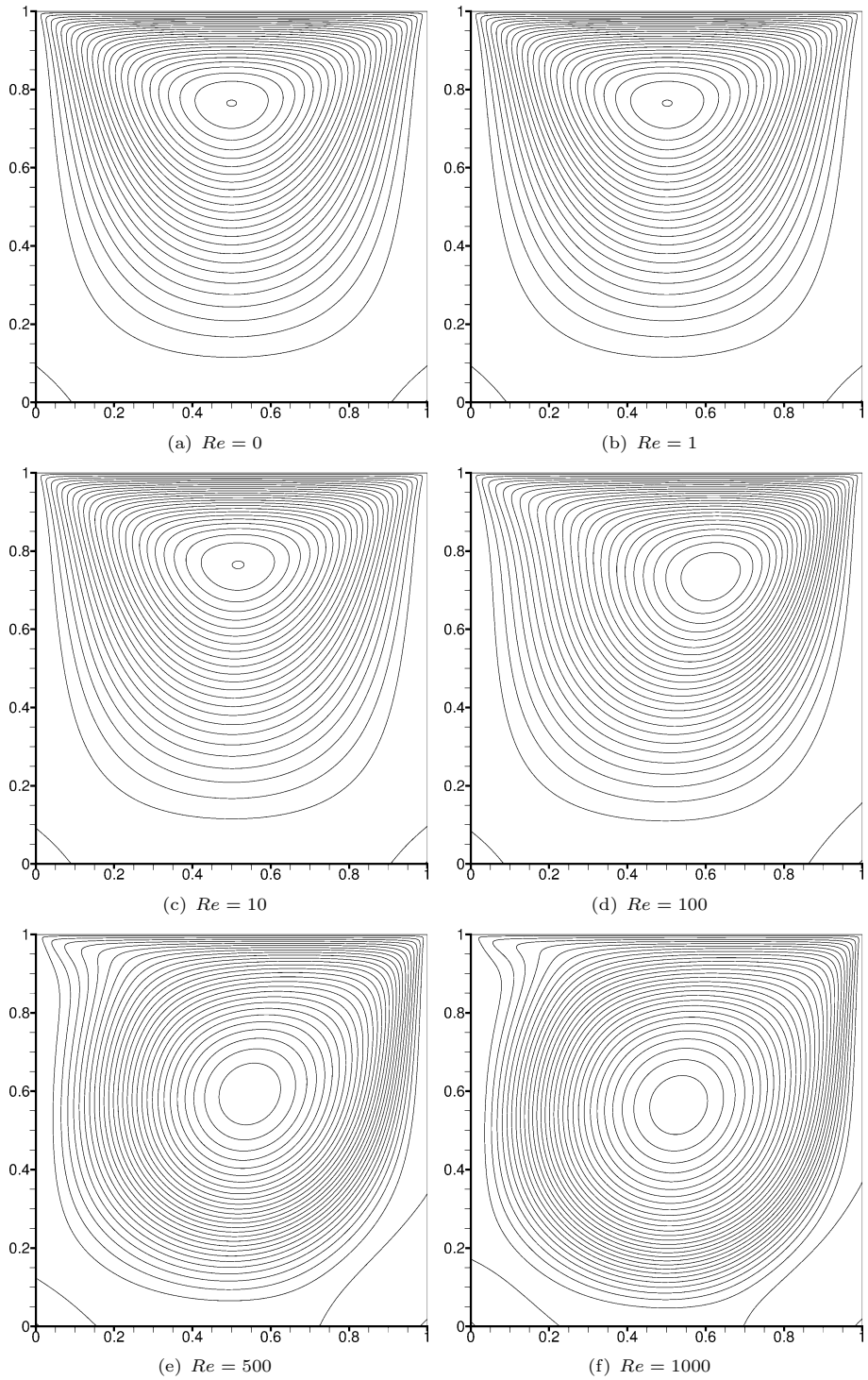

(a) $Re = 0$ (b) $Re = 1$

(c) $Re = 10$ (d) $Re = 100$

(e) $Re = 500$ (f) $Re = 1000$

Figure 1: Streamlines in Newtonian flow ($Bn = 0$), plotted at intervals of 0.004 starting from zero.

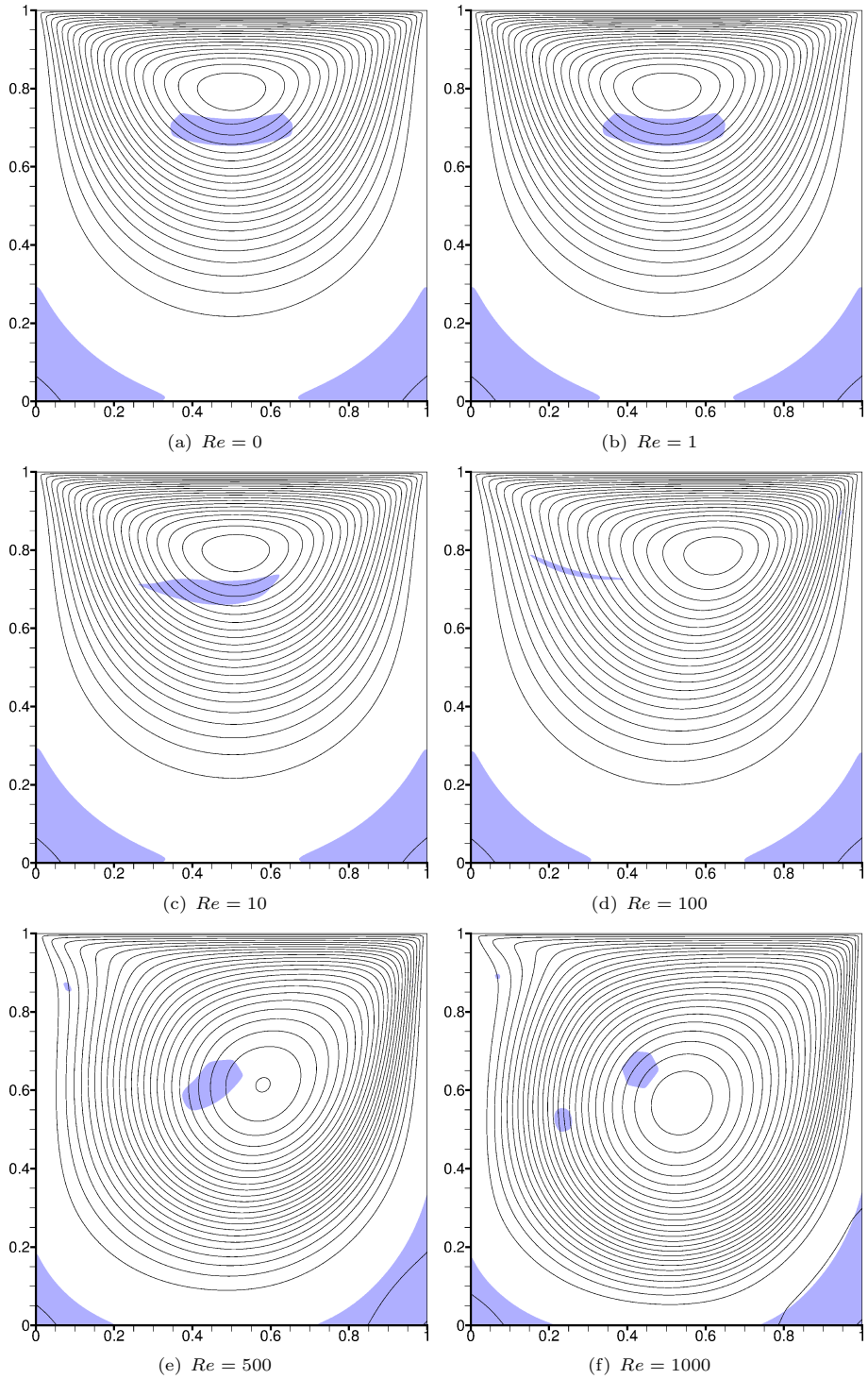

(a) $Re = 0$ (b) $Re = 1$

(c) $Re = 10$ (d) $Re = 100$

(e) $Re = 500$ (f) $Re = 1000$

Figure 2: Streamlines in Bingham flow for Bn = 1, plotted at intervals of 0.004 starting from zero. Unyielded areas ($\tau < Bn$) are shown shaded.

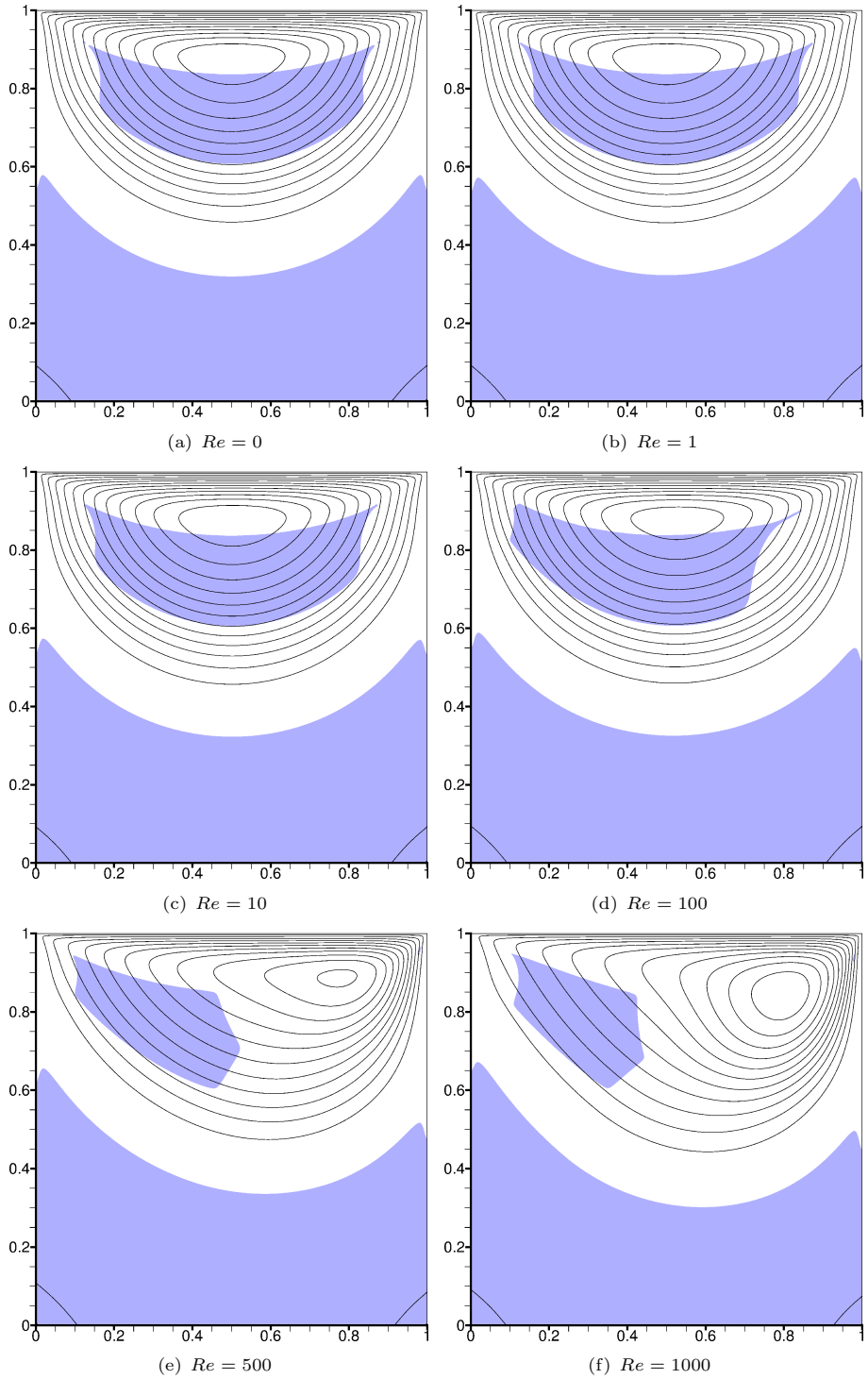

(a) $Re = 0$ (b) $Re = 1$

(c) $Re = 10$ (d) $Re = 100$

(e) $Re = 500$ (f) $Re = 1000$

Figure 3: Streamlines in Bingham flow for Bn = 10, plotted at intervals of 0.004 starting from zero. Unyielded areas ($\tau < Bn$) are shown shaded.

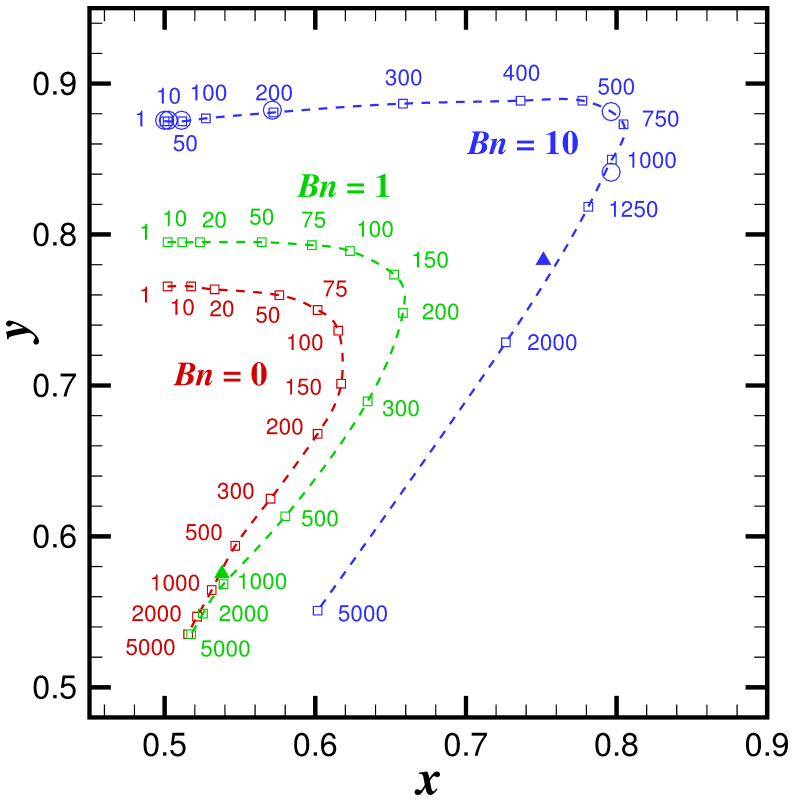

Figure 4: The position of the vortex centre, for various values of Re and Bn. The results of the present study are shown as empty squares (□), with the Reynolds number written next to each square. The results of Vola et al [13] (Re = 1000: Bn = 1, 10) and of Prashant and Derksen [14] (Re = 0.5, 10, 50, 200, 600, 1000: Bn = 10), are indicated by filled triangles (▲) and empty circles (◯), respectively.

corners; these are in fact an artifact of the Papanastasiou regularisation which treats all of the material as a fluid. On the other hand, the unyielded region that is close to the vortex centre and does not touch the cavity walls is clearly not motionless. This can be seen from the streamlines' spacing inside these regions, which shows that the velocity is non-zero. These regions move as solid bodies. The fact that the flow is steady-state means that these "solid bodies" lose mass on their downstream boundary at a rate equal to that at which they gain mass on their upstream boundary, so that their location and size remains fixed in time. In other words, a fluid particle "solidifies" on entry to this region, and following the streamline path it later exits the region, at which point it becomes "fluid" again.

The position of the vortex centre for various Re and Bn numbers is shown in Figure 4. The present results are close to those of Vola et al [13] and Prashant and Derksen [14], except for the (Re=1000, Bn=10) case, where there is is some discrepancy between the present results and those of Vola et al. However, the agreement is very good with the results of Prashant and Derksen [14]. Figure 4 shows that there is a trend in which, as the Reynolds number increases, the main vortex initially moves towards the downstream side wall, and then, beyond a certain Reynolds number, it moves towards the cavity centre. As Bn increases, these phenomena are postponed to higher Reynolds numbers and, in addition, the vortex moves higher towards the lid, as the bottom of the cavity becomes filled with "solid" material and the flow region is restricted.

Tables 1 – 2 contain results on the x-component of velocity along the vertical centreline, for

Table 1: Values of the x-component of velocity along the vertical centreline for $Re = 1000, Bn = 1$. The order of grid convergence, q, is defined by Eq. (10).

grid	128×128	256×256	512×512	512×512	512×512	q
y	$M = 400$	$M = 400$	$M = 400$	$M = 200$	$M = 100$	
1.000	1.00000	1.00000	1.00000	1.00000	1.00000	-
0.990	0.83434	0.83687	0.83734	0.83734	0.83733	2.41
0.980	0.68125	0.68471	0.68593	0.68592	0.68591	1.51
0.960	0.46586	0.47143	0.47274	0.47273	0.47271	2.09
0.930	0.34382	0.34918	0.35050	0.35048	0.35046	2.02
0.900	0.30799	0.31269	0.31389	0.31387	0.31383	1.97
0.850	0.26486	0.26900	0.27007	0.27005	0.27000	1.95
0.800	0.21625	0.21965	0.22054	0.22053	0.22052	1.93
0.700	0.11957	0.12136	0.12184	0.12186	0.12190	1.90
0.600	0.03123	0.03185	0.03203	0.03205	0.03207	1.78
0.500	-0.05486	-0.05520	-0.05526	-0.05523	-0.05517	2.55
0.400	-0.14093	-0.14186	-0.14206	-0.14204	-0.14201	2.21
0.300	-0.23422	-0.23608	-0.23652	-0.23650	-0.23647	2.08
0.220	-0.30655	-0.30973	-0.31051	-0.31049	-0.31046	2.02
0.180	-0.32376	-0.32847	-0.32969	-0.32969	-0.32968	1.95
0.140	-0.29831	-0.30398	-0.30552	-0.30555	-0.30559	1.88
0.100	-0.23360	-0.23851	-0.23989	-0.23994	-0.24002	1.82
0.050	-0.13004	-0.13274	-0.13354	-0.13359	-0.13367	1.76
0.000	0.00000	0.00000	0.00000	0.00000	0.00000	-

Table 2: Values of the x-component of velocity along the vertical centreline for $Re = 1000, Bn = 10$. The order of grid convergence, q, is defined by Eq. (10).

grid	128×128	256×256	512×512	512×512	512×512	q
y	$M = 400$	$M = 400$	$M = 400$	$M = 200$	$M = 100$	
1.000	1.00000	1.00000	1.00000	1.00000	1.00000	-
0.990	0.78014	0.78237	0.78283	0.78295	0.78318	2.28
0.980	0.58320	0.58552	0.58662	0.58683	0.58719	1.07
0.960	0.28798	0.29236	0.29359	0.29400	0.29476	1.83
0.920	0.03885	0.04330	0.04480	0.04544	0.04665	1.57
0.880	-0.02432	-0.02168	-0.02059	-0.02003	-0.01896	1.29
0.850	-0.03940	-0.03904	-0.03892	-0.03850	-0.03769	1.59
0.750	-0.05502	-0.05520	-0.05520	-0.05493	-0.05439	8.26
0.650	-0.06670	-0.06763	-0.06802	-0.06771	-0.06715	1.25
0.580	-0.07537	-0.07575	-0.07589	-0.07576	-0.07549	1.52
0.540	-0.07895	-0.07926	-0.07934	-0.07908	-0.07857	1.89
0.500	-0.07775	-0.07911	-0.07949	-0.07911	-0.07838	1.81
0.460	-0.06274	-0.06498	-0.06561	-0.06550	-0.06529	1.84
0.420	-0.03891	-0.04167	-0.04257	-0.04274	-0.04303	1.61
0.380	-0.01636	-0.01878	-0.01977	-0.02021	-0.02102	1.27
0.340	-0.00363	-0.00390	-0.00429	-0.00505	-0.00648	-0.52
0.300	-0.00096	-0.00087	-0.00084	-0.00164	-0.00318	1.60
0.200	-0.00043	-0.00043	-0.00042	-0.00084	-0.00165	0.92
0.100	-0.00021	-0.00020	-0.00020	-0.00040	-0.00080	0.68
0.000	0.00000	0.00000	0.00000	0.00000	0.00000	-

$Re = 1000$ and Bn = 1 and 10, respectively. These were obtained on various grids and with various values of M, estimated at the selected points using linear interpolation. The points selected differ for the various Bn numbers, and they were chosen so as to provide good descriptions of the profiles. The results listed can be used to check grid convergence and "M–convergence", i.e. whether an M–independent solution has been reached. The exponent q in Tables 1 and 2 is the order of grid convergence, defined as (see [12])

$$q \equiv \frac{\log\left(\frac{u_{256}-u_{128}}{u_{512}-u_{256}}\right)}{\log(2)} \tag{10}$$

where the subscripts denote the grid where u was calculated. Since the equations were discretised using 2$^{\text{nd}}$ order accurate central differences, q should equal 2.

Table 1 shows that, for $Bn = 1$, the method indeed exhibits a 2$^{\text{nd}}$ order rate of convergence with grid refinement, with the exponent q being very close to 2. From the difference between the solutions of the two finest grids and the $q = 2$ order of convergence, a discretisation error of the order of 0.02 is estimated. The difference between using $M = 200$ and $M = 400$ is very small, meaning that grid coarseness appears to be a larger source of error than the magnitude of M in this particular case.

From Table 2, it is deduced that for $Bn = 10$, the order of grid convergence is now clearly below 2, and in particular the mean value of the exponent q is just over 1.5 (excluding extreme values). This is a sign that the grid is not fine enough. The discretisation error on grid 512×512 appears to be about 0.5%, assuming 2$^{\text{nd}}$ order convergence. The difference between using different M indices is also larger. These observations lead to the conclusion that finer grids and larger values of M should be used with larger Bingham numbers.

Finally, Figure 5 shows the reduction of the algebraic residuals as a function of the computational effort for $Re = 1000$ and Bn = 1 and 10, as typical examples. The ordinate is the the L^∞-norm of the residual vector of the $x-$momentum equations,

$$\|r\|_\infty \; = \; \max_{P=1,\ldots,N} \{|r_P|\} \; , \tag{11}$$

where r_P is the residual, expressed per unit volume, of the $x-$momentum equation of control volume P and N is the total number of control volumes in the grid. The computational effort is measured in equivalent fine-grid SIMPLE iterations. For the multigrid cases, the number of equivalent fine-grid SIMPLE iterations is obtained by multiplying the number of cycles by the number of fine-grid SIMPLE iterations that cost computationally the same as a single cycle. In particular, n_C cycles of type W(ν_1, ν_2)–ν_3 cost approximately the same as $n_S = n_C \cdot [2(\nu_1 + \nu_2) + \nu_3]$ SIMPLE iterations on the finest grid. For example, one W(6,6)-10 cycle costs the same as 34 fine-grid SIMPLE iterations. It should be noted that the cost of restriction and prolongation is omitted in this calculation, since it is very small compared to the cost of the SIMPLE iterations, especially if one considers that the numbers of pre- and post- smoothing iterations are large, and fine-grid iterations are also carried out between cycles. Therefore, multigrid and single-grid convergence rates are directly comparable in Figure 5. The SIMPLE underrelaxation factors were chosen differently in the multigrid and single-grid cases, in order to make the solvers more efficient in each case.

Figure 5 also shows that the multigrid procedure greatly accelerates the convergence of SIMPLE. One can notice that as the grid becomes finer, the multigrid convergence slows down in general - this is not typical multigrid behaviour, and is explained by the fact that the present multigrid method contains single-grid features, as described in Section 3. For Bn = 10, on the 256×256 and 512×512 grids the procedure converges fast at the initial stages, due to a good initial guess, but slows down at later stages of iteration. The convergence rates decrease as Bn increases, and are significantly worse than those typically exhibited in Newtonian flows.

5 CONCLUSIONS

The present work has shown that the finite volume method, coupled with the SIMPLE algebraic solver in a multigrid framework, can be easily adapted to use the Papanastasiou regularisation for the simulation of Bingham flows for a wide range of Reynolds and Bingham numbers. The method has been tested on the lid-driven cavity problem, yielding results that agree with

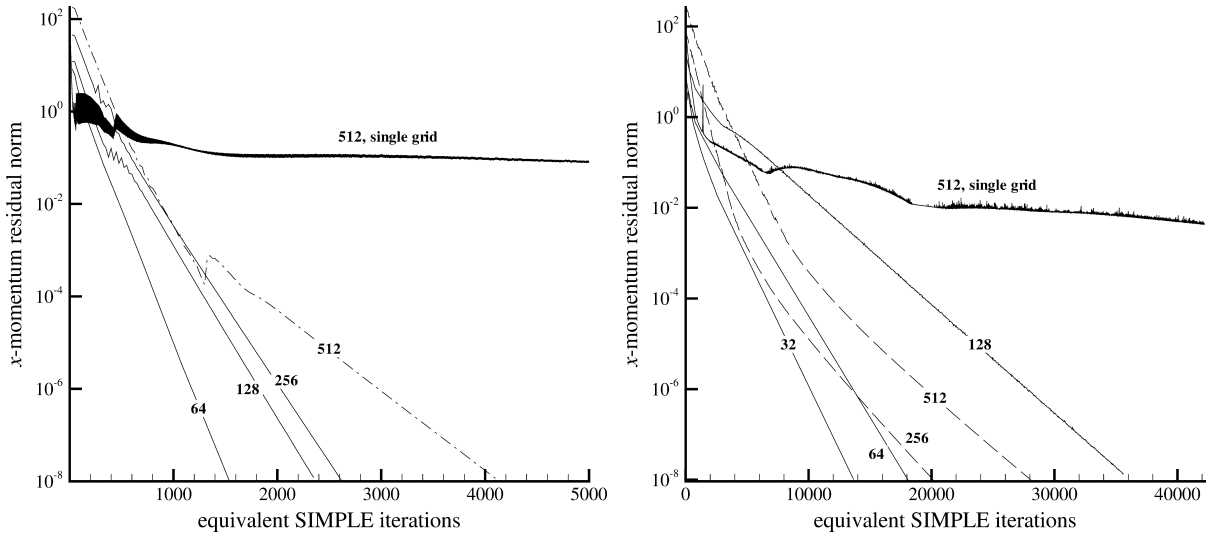

(a) Re = 1000; Bn = 1

(b) Re = 1000; Bn = 10

Figure 5: Maximum x-momentum residual per unit volume (11) versus computational effort, for Re = 1000 and Bn = 1 and 10. The results refer to the SIMPLE/multigrid algebraic solver, using the 8×8 as the coarsest grid, except for a single-grid case which is indicated on each figure. The number on each curve indicates the finest grid (n means that the finest grid has $n \times n$ control volumes). The algebraic solver parameters are the following (see Section 3 for definitions): For Bn = 1, W(5,5)-5 cycles, α_{MG} = 1.0, a_u = 0.7, and a_p = 0.02 (multigrid) or 0.2 (single grid). For Bn = 10, W(6,6)-10 cycles, α_{MG} = 0.9, and $\{a_u, a_p\}$ = {0.5, 0.02} (multigrid) or {0.7, 0.2} (single grid). On each grid, the solution of the immediately coarser grid was used as the initial guess.

those of previously published works, which employed different solution methods. It is observed that as the Bingham number increases, it becomes more difficult for the SIMPLE/multigrid method to solve the algebraic system that results from the finite volume discretisation. Also, to maintain a certain level of accuracy, the Papanastasiou exponent M and the grid density should increase as the Bingham number increases. This causes additional difficulties to the algebraic solver. The multigrid framework is necessary for the solver to be efficient, as the convergence of SIMPLE alone is too slow. The method is currently being tested on yet higher Bn numbers.

ACKNOWLEDGEMENTS

This work was supported by the Cyprus Research Promotion Foundations Framework Programme for Research, Technological Development and Innovation 2009-2010 (DESMI 2009-2010), co-funded by the Republic of Cyprus and the European Regional Development Fund, and specically under Grant ΑΕΙΦΟΡΙΑ/ΦΥΣΗ/0609(BIE)/15.

REFERENCES

[1] T.C. Papanastasiou, Flows of materials with yield. *Journal of Rheology*, **31**, 385–404, 1987.

[2] A. Syrakos, A. Goulas, Finite volume adaptive solutions using SIMPLE as smoother. *International Journal for Numerical Methods in Fluids*, **52**, 1215–1245, 2006.

[3] A. Syrakos, G.C. Georgiou, A.N. Alexandrou, Solution of the square lid-driven cavity flow of a Bingham plastic using the finite volume method. *Journal of Non-Newtonian Fluid Mechanics*, **195**, 19–31, 2013.

[4] P. Neofytou, A 3rd order upwind finite volume method for generalised Newtonian fluid flows. *Advances in Engineering Software*, **36**, 664–680, 2005.

[5] S.V. Patankar, D.B. Spalding, A calculation procedure for heat, mass and momentum transfer in three-dimensional parabolic flows. *International Journal of Heat and Mass Transfer*, **15**, 1787–1806, 1972.

[6] O. Turan, N. Chakraborty, R.J. Poole, Laminar natural convection of Bingham fluids in a square enclosure with differentially heated side walls. *Journal of Non-Newtonian Fluid Mechanics*, **165**, 901–913, 2010.

[7] P. Neofytou, D. Drikakis, Effects of blood models on flows through a stenosis. *International Journal for Numerical Methods in Fluids* **43**, 597–635, 2003.

[8] P. Neofytou, D. Drikakis, Non-Newtonian flow instability in a channel with a sudden expansion. *Journal of Non-Newtonian Fluid Mechanics*, **111**, 127–150, 2003.

[9] P.R. de Souza Mendes, M.F. Naccache, P.R. Varges, F.H. Marchesini, Flow of viscoplastic liquids through axisymmetric expansions-contractions. *Journal of Non-Newtonian Fluid Mechanics*, **142**, 207–217, 2007.

[10] M.F. Naccache, R.S. Barbosa, Creeping flow of viscoplastic materials through a planar expansion followed by a contraction. *Mechanics Research Communications*, **34**, 423–431, 2007.

[11] A. Syrakos, A. Goulas, Estimate of the truncation error of finite volume discretization of the NavierStokes equations on colocated grids. *International Journal for Numerical Methods in Fluids*, **50**, 103–130, 2006.

[12] J.H. Ferziger, M. Perić, *Computational methods for fluid dynamics, 3rd Edition*. Springer, 2002.

[13] D. Vola, L. Boscardin, J.C. Latché, Laminar unsteady flows of Bingham fluids: a numerical strategy and some benchmark results. *Journal of Computational Physics*, **187**, 441–456, 2003.

[14] Prashant, J.J. Derksen, Direct simulations of spherical particle motion in Bingham liquids. *Computers and Chemical Engineering*, **35**, 1200–1214, 2011.

[15] M. Fortin, R. Glowinski, *Augmented Lagrangian Methods: applications to the numerical solution of boundary-value problems*. North-Holland, 1983.

[16] E.J. O'Donovan, R.I. Tanner, Numerical study of the Bingham squeeze film problem. *Journal of Non-Newtonian Fluid Mechanics*, **15**, 75–83, 1984.